

Current-induced vortex motion and the vortex-glass transition in $\text{YBa}_2\text{Cu}_3\text{O}_y$ films

T. Nojima, A. Kakinuma, and Y. Kuwasawa

Department of Physics, Faculty of Science, Chiba University, 1-33 Yayoicho, Inage-ku, Chiba 263, Japan

(Received 22 July 1997)

Measurements of current-voltage characteristics have been performed on $\text{YBa}_2\text{Cu}_3\text{O}_y$ films for two components of electric fields in the ab plane, E_x and E_y , in magnetic fields of the form $(H_0, H_0, \delta H_0)$, where $x \parallel$ the current density J , $z \parallel$ the c axis, and $\delta \ll 1$. The simultaneous measurements of E_x and E_y under these conditions make it possible to analyze the situation of the vortex motion due to the Lorentz force. Our results indicate that vortices move as long-range correlated lines only below the glass transition temperature in a low-current limit. We also show that applying high-current density destroys line motion and induces a structural change of vortex lines in the glass state. [S0163-1829(97)50846-0]

Recently it has been widely recognized that there exists a phase transition¹⁻⁵ in the vortex system of high- T_c superconductors. In a clean system with very weak flux pinning centers, the transition is predicted to be a first order transition from a vortex liquid to an Abrikosov vortex lattice.¹⁻³ On the other hand, in a dirty system with random pointlike or line (plane)-like (correlated) disorders, the transition has been postulated to be a second-order phase transition to a vortex-glass⁴ (VG) or a Bose glass⁵ (BG) state, depending on the type of disorder. Experimentally, strong evidence for the VG transition was presented by the scaling analysis of current-voltage (I - V) characteristics in $\text{YBa}_2\text{Cu}_3\text{O}_{7-\delta}$ (YBCO) films⁶ or the SQUID picovoltmetry in twinned YBCO crystals,⁷ indicating the disappearance of linear resistance at a glass transition T_g . Until now, many experimental data have supported the existence of a glass transition,⁶⁻¹⁰ although there is still some controversy as to whether the glass phase is VG or BG when an applied magnetic field H is parallel to the c axis (parallel to extended defects like twin planes or screw dislocations) for YBCO films.¹¹⁻¹³

After the glass transition has become an accepted concept, the dynamics of vortices both in liquid and glass states remains attractive subjects. According to the glass transition theories,⁴ long-range correlation between vortices establishes in all directions at a glass transition temperature T_g with diverging correlation length ξ_g , which varies as $\xi_g \sim |T - T_g|^{-\nu}$ with a static critical exponent ν . This implies that in a liquid state with a finite length of ξ_g vortices correlate only in a short range even in the direction along the applied field. So then, vortices in a liquid state cannot move as a line by applying current, and line motion becomes possible at $T = T_g$. In a glass state, the dissipation is considered to be described by the composition of the vortex loop excitations with a length scale L , which is a decreasing function of current.⁴ When L becomes shorter than ξ_g due to increasing current, the correlated motion of the vortex line may be destroyed again. In order to deeply understand the nature of the vortex system in both glass and liquid phases, one may need to investigate the motion of the vortices directly as a function of temperature and current. This is the motivation of our work.

The vortex correlation along magnetic field direction has been studied in several experiments using the dc flux trans-

former geometry.¹⁴⁻¹⁹ For clean YBCO (Ref. 15) and $\text{Bi}_2\text{Sr}_2\text{CaCu}_2\text{O}_8$ (BSCCO) single crystals,¹⁶ the disappearance of this correlation just at the melting transition temperature has been observed. For twinned YBCO crystals¹⁷ and heavy ion irradiated crystals of YBCO (Ref. 18) and BSCCO (Ref. 19), the existence of correlated vortex lines in the liquid phase in H parallel to correlated disorders has been argued using the BG theory.^{5,20} Similar investigations should be performed for systems which show the VG transition, such as YBCO films.

In this paper, we present measurements of current-voltage (I - V) characteristics on YBCO films for both longitudinal and transverse voltage in the ab plane for H with a particular condition near $H \perp c$ as described below. This observation allows us to examine the direction of the vortex motion directly as a function of temperature T and current density J . In the experiments, we demonstrate that the vortices, which mainly move in the ab plane at temperatures far above T_g reflecting the absence of a correlation along the field direction, change the direction of their motion with decreasing T , and finally move along the macroscopic Lorentz force (almost parallel to the c axis) below T_g in a low-current limit. This result is consistent with the idea that vortices form lines along the H direction at T_g as predicted in the VG theory. We also find that line motion in the glass state is destroyed by applying J larger than a characteristic density J_d . A comparison between the size of the vortex loop excitation and the correlation length or between the barrier energy of the loop excitation and the thermal energy provides a qualitative explanation to the temperature dependence of J_d .

The relation between the directions of current density J , magnetic field H , and the c axis used in the measurements is shown in Fig. 1. The component of the applied H along the ab plane makes an angle of 45° with J direction (x axis) and the component along the c axis (z axis) is very small with an angle of $\alpha = 0-5^\circ$. This configuration is very similar to that used for the study of the vortex motion in the multilayer system discussed previously.²¹ In this experimental condition, the magnetic flux density $\mathbf{B} = (B_0, B_0, \delta B_0)$ with $\delta \leq 0.1$ and $\mathbf{J} = (J, 0, 0)$. Then the Lorentz force $\mathbf{F}_L = \mathbf{J} \times \mathbf{B}$ with the components $(0, -\delta JB_0, JB_0)$ moves the vortices with a velocity $\mathbf{v} = (0, -v_y, v_z)$. Here we use $v_y, v_z > 0$. This motion

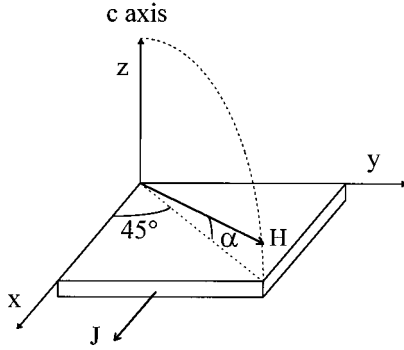


FIG. 1. A schematic drawing for the experimental condition, showing the relationship between the directions of the c axis, the magnetic field H , and the current density J .

will yield an electric field $\mathbf{E}=(E_x, E_y, E_z)=(v_z B_0 + \delta v_y B_0, -v_z B_0, -v_y B_0)$. If the vortices form lines with a long-range correlation along the \mathbf{B} direction, they move along \mathbf{F}_L for a small enough current. In this case, $|E_y|$ almost equal to $|E_x|$ would be observed, since $v_y \ll v_z$ ($|F_y| \ll |F_z|$) and $\delta \ll 1$. If the correlation of the vortices are destroyed by large thermal fluctuations or high J on the other hand, uncorrelated parts of the vortices may move as pancake vortices in each Cu-O layer.^{22,23} In such a case, the observed $|E_y|$ would be much smaller than $|E_x|$ since v_z is suppressed and v_y becomes noticeable. Therefore, the simultaneous measurements of E_x and E_y as a function of T and J make it possible to investigate the onset of the correlated motion of the vortices.

The YBCO films used in this study were prepared by a laser ablation method on the (100) surface of YSZ (yttrium stabilized zirconium) single crystals. The critical temperature determined by the peak of dR/dT is typically 89.6 K and the critical current density at 77 K in zero applied field is more than 1×10^6 A/cm². The x-ray diffraction measurements show that the films are predominantly c -axis up. The full-width half maximum (FWHM) of a rocking curve of the (005) reflection is $\approx 0.6^\circ$. The sample with the thickness of $0.35 \mu\text{m}$ was patterned to a strip with dimension of $270 \mu\text{m} \times 1000 \mu\text{m}$ by chemical etching. The current leads were attached to the Au pads deposited on the film surface with contact resistance less than 1Ω . For the measurements of two kinds of voltage components, two pairs of indium electrodes with a width of $\approx 50 \mu\text{m}$ were attached to both sides of the strip as shown in the inset of Fig. 2.

The experimental configuration as shown in Fig. 1 was produced by making a sample holder which can rotate α around the diagonal line of the xy sample plane in a magnetic field, keeping an angle between the in-plane component of H and J at 45° . The angular resolution of α is better than 0.2° . It should be noted that the transverse electric field measured consists of two variables, the first being E_y coming from the vortex motion along the z axis due to the Lorentz force as mentioned above and the second being E_{Hall} from the Hall effect induced by the c -axis component of H or the motion of the pancake vortices along the x axis, although E_{Hall} is very small in comparison with E_y in the critical region near T_g . In order to derive E_y only, we performed the same measurements in reverse magnetic fields. After averag-

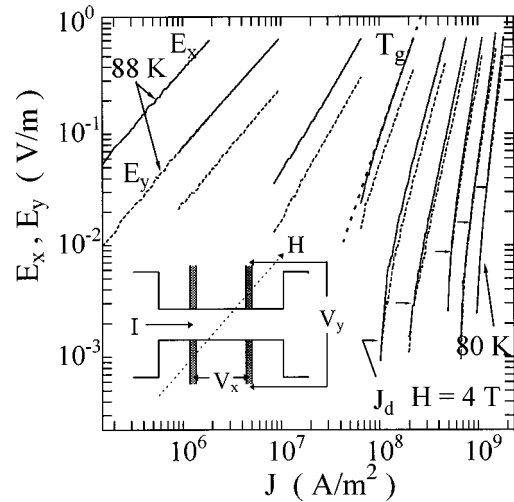


FIG. 2. E - J characteristics around T_g for two electric fields, E_x (solid line) and E_y (dashed line), at $H=4$ T for $\alpha=5^\circ$. Temperature range is from 88 K to 80 K in steps of 1 K. The inset shows the sample configuration with an indication of the electrodes for the voltage measurements.

ing the two kinds of data for both signs of magnetic fields, the Hall voltage was canceled out, since $E_{\text{Hall}}(H) = -E_{\text{Hall}}(-H)$ and $E_y(H) = E_y(-H)$.

Figure 2 shows two typical sets of E - J characteristics (E_x - J and E_y - J) around the glass transition in $H=4$ T at $\alpha=5^\circ$. The measurements were performed also in $H=6$ and 8 T at $\alpha=5^\circ$ and in $H=4$ T at $\alpha=0^\circ$. The similar types of $E_{x,y}$ - J curves are observed for all the above conditions. With decreasing T , the positive curvature of $\ln E_x$ - $\ln J$ curve changes to a negative one below $T=T_g$ (thick dashed line in Fig. 2). As reported by many authors,^{6,9,13} this change is regarded as a standard behavior of the vortex glass transition. Indeed the scaling collapses are obtained by taking $T_g=85$ K with the static exponent $\nu=1.5$ and dynamic exponent $z=4.0$, which are derived from the slope of the dashed line $(z+1)/2$ in Fig. 2 and the fitting of $\rho_x=E_x/J$ in the linear region near T_g to $\rho_x \sim (T/T_g - 1)^{\nu(z-1)}$. In Fig. 2, we note that two curves of $E_x(J)$ and $E_y(J)$ approach with decreasing T and have the same trace in a low-current region below T_g . In our experimental condition, E_y is given by the z component of the vortex motion, and E_x is given by both the z component and y component. Since the direction of the macroscopic Lorentz force \mathbf{F}_L is also nearly the z direction, the identification of $|E_x|$ and $|E_y|$ implies that the vortices move along \mathbf{F}_L across the ab plane. Therefore, the results lead to the conclusion that the vortices form (approximately straight) lines extending along the direction of applied magnetic field at T_g , and move as lines in a low-current limit below T_g , as in ordinary anisotropic superconductors. If the vortices formed pancakelike²² or stepwise²³ configurations even at T_g due to weak or short-range correlation originating from the layer structure, their motions would result in $|E_y| \ll |E_x|$ because the easy motion of vortices is along the y direction.

In Fig. 3, we plot the ratio of $|E_y/E_x|$ in the low voltage region below $E_x=2 \times 10^{-3}$ V/m in $H=4$ T as a function of T . With decreasing T , $|E_y/E_x|$ starts to increase from zero around T^* , below which the scaling power law of resistivity

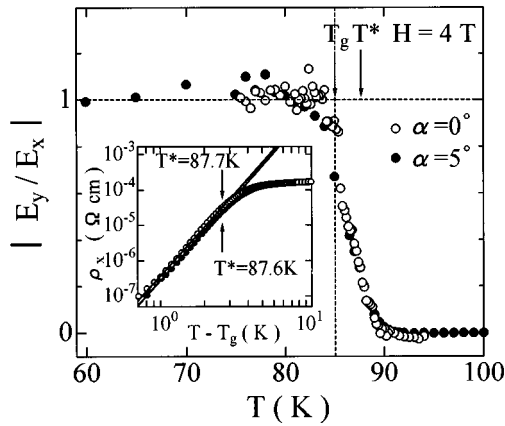


FIG. 3. Plots of the ratio $|E_y/E_x|$ as a function of T at $H=4$ T for $\alpha=5^\circ$ (solid circles) and $\alpha=0^\circ$ (open circles). The inset shows $\rho_x=E_x/J$ in the Ohmic regime as a function of T/T_g-1 for the same conditions. The critical region starts at T^* .

$\rho_x \sim |T-T_g|^{\nu(z-1)}$ as shown in the inset of Fig. 3, and the ratio transfers to 1 at $T \approx T_g$. The behavior of the ratio indicates a developing process of the vortex lines as follows: (1) At high temperature far from T_g , the vortices move only in the CuO plane without coupling along the H direction ($E_y=0$). (2) The vortices start to correlate with each other around T^* and the correlated parts of vortices extend with decreasing T . (3) They finally become lines at $T=T_g$. In the theory of the vortex glass transition, the remarkable correlation of vortices begins in the critical state below T^* and the establishment of long-range order in all directions occurs at T_g with diverging glass correlation length $\xi_g \sim |T-T_g|^{-\nu}$. The process obtained from our experimental results is consistent with the idea of the vortex glass transition and suggests the existence of a second-order phase transition at T_g .

Recent transport measurements using the dc flux transformer geometry in twinned YBCO single crystals have indicated that a certain temperature region $T_g < T < T_{th}$, where vortices move as lines, exists in a liquid phase for $H \parallel c$.^{14,17} T_{th} decreases with the increase of sample thickness. As explained in the Bose glass model,^{5,20} this line-liquid region is caused by the faster development, than that in the ab plane, of the correlation length along the twin-boundary pinning.¹⁷ In our case, the applied field is highly tilted from the c axis and the twin planes may not work as the vortex pinning sites. If vortices are pinned by pointlike disorder, the coincidence of line formation and glass transition in our experiment is reasonable since the development of the correlation is expected to be almost isotropic.

At low temperatures below T_g , the E_x - J curve and the E_y - J curve, both of which are identified at a low J , separate above a well-defined current density J_d (denoted by arrows in Fig. 2). In Fig. 4, we also plot the representative data below T_g for (a) $H=4$ T and (b) $H=8$ T. These linear scale plots allow us to see the separation more clearly. (Here J_d was defined as a current density at which $|E_y/E_x|$ becomes equal to 0.85.) Since the relation $|E_y| < |E_x|$ at the same J means that the motion of vortices along the ab plane is remarkable, the separation indicates that the vortex line is deformed to steplike or pancakelike configuration. J_d is a characteristic current for the current-induced deformation, which

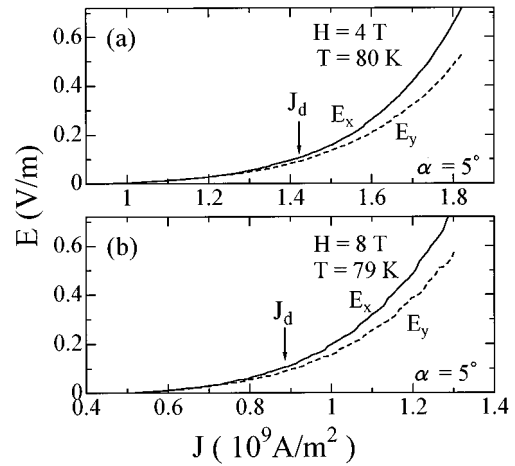


FIG. 4. $E_x(J)$ and $E_y(J)$ in a linear scale for $\alpha=5^\circ$ (a) at $T=80.0$ K in $H=4$ T and (b) at $T=79.0$ K in $H=8$ T. The arrows show the current density J_d defined as $|E_x/E_y|=0.85$.

contrasts with the thermal fluctuation-induced effect above T_g .

In Fig. 5, the values of J_d in $H=4, 6$, and 8 T at $\alpha=5^\circ$ and in $H=4$ T at $\alpha=0^\circ$ are plotted as a function of T/T_g . In the vicinity of $T/T_g=1$, $J_d(T)$ at all fields is scaled by T/T_g and its curve has a positive curvature as indicated in the inset of Fig. 5. At low temperatures far below T_g , $J_d(T)$ curves are dependent on H and show a negative curvature. From these results, we infer two different processes for the current-induced destruction of the vortex line, depending on temperature range.

In order to understand the behavior of $J_d(T)$, we now consider the dissipation process by expansion of an excited vortex loop.⁴ Supposing that the loop excitation is composed of a displacement of vortex lines with an amplitude L_\perp over the line length L_\parallel , the elastic energy cost due to the excitation is given by $\sim Y L_\perp^2 / L_\parallel$ and the energy gain from the current by $\sim J \Phi_0 L_\perp L_\parallel$. Here Y is a stiffness coefficient and Φ_0 is the flux quantum. According to Ref. 4 and the references therein, L_\perp is numerically found to scale as $\sim L_\parallel^\zeta$ with

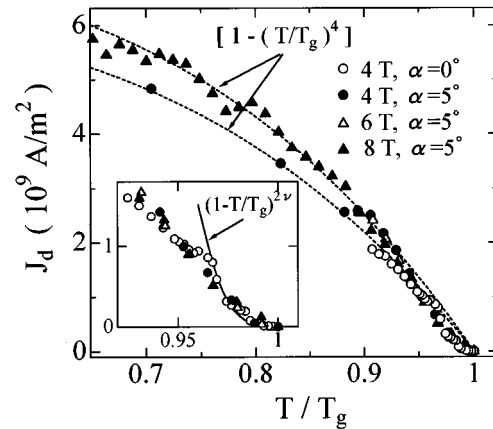


FIG. 5. Temperature dependence of J_d . The dashed lines are fits to the data with $J_d \sim 1 - (T/T_g)^4$. Inset: Expanded view of the same data of $J_d(T)$ around $T/T_g=1$. The solid line is a fit to the data with $J_d \sim (1 - T/T_g)^{2\nu}$.

an exponent $\zeta \sim 0.6$ in a disorder-dominated pinned phase. Then the line length $L_{\parallel J}$ and the displacement $L_{\perp J}$, which are significant in the presence of the applied current density J , are obtained by balancing the two energies as follows:

$$L_{\parallel J} \sim (\Upsilon/J\Phi_0)^{1/(2-\zeta)} \quad \text{and} \quad L_{\perp J} \sim (\Upsilon/J\Phi_0)^{\zeta/(2-\zeta)}. \quad (1)$$

Through the loop excitation the vortex lines have to pass over a free energy barrier $B_L \sim \Delta(L_{\perp J})^\Psi$ with an exponent Ψ .⁴ The rate Γ of the thermal nucleation of the vortex loop is given by

$$\Gamma \sim \exp\left[-\left(\frac{B_L}{k_B T}\right)\right] = \exp\left[-\left(\frac{J_T}{J}\right)^\mu\right], \quad (2)$$

with $\mu = \Psi\zeta/(2-\zeta)$ and $J_T \sim (\Upsilon/\Phi_0)(\Delta/k_B T)^{1/\mu}$. From Eqs. (1) and (2), two kinds of current scales, J_F and J_T , are defined: $J_F = \Upsilon/(\Phi_0 \xi_{g\parallel}^{2-\zeta})$ is a current density at which the loop size $L_{\parallel J}$ in Eq. (1) becomes comparable to the correlation length $\xi_{g\parallel}$ along H . J_T is one at which B_L is comparable to $k_B T$. When the applied J is larger than J_F , the nonactivated loop excitation with a smaller size than $\xi_{g\parallel}$ may result in the destruction of correlated vortex motion or cutting of the vortex lines. When J approaches J_T , the frequent occurrence of thermally activated phase slip may also destroy the correlation. At low temperatures far below T_g , J_F is much smaller than J_T ,⁴ and the correlation length, which may be of order the Larkin-Ovchinnikov length²⁴ at least, is expected to be T independent for YBCO films.^{8,9} In this case, the observable current density for the vortex line deforma-

tion may be J_F which is proportional to Υ with an approximate $1 - (T/T_g)^4$ temperature dependence.^{4,8} In the critical region near T_g , $J_T \approx J_F$ and it scales as $(\text{length})^{1-D}$ with a dimension D .⁴ In this case, we expect that the observed deformation current is proportional to $\xi_g^{-2} \sim |1 - T/T_g|^{2\nu}$. The dashed lines in Fig. 5 and the solid line in the inset are the fits of the deformation current $J_d(T)$ by using the two relations in temperature regions far below T_g and close to T_g , respectively. The agreement supports the existence of the vortex glass phase and the dissipation process through the loop excitation.

In conclusion, having performed simultaneous measurements of the E - J characteristics for longitudinal and transverse electric fields in magnetic fields with the particular direction, we found that the curvature change in $\ln E$ - $\ln J$ curves and the onset of the vortex motion as a line coincide at the same temperature T_g . This indicates that the vortex line formation is established with the vortex glass transition, which is consistent with the theoretical prediction. In the glass state, line motion is destroyed by applying a current density larger than J_d . The temperature dependence of J_d can be qualitatively explained by considering the dissipation process due to the vortex loop excitation, which suggests the existence of the vortex glass phase.

The authors would like to thank I. Kameyama and K. Onabe for their help in the measurements and the sample preparation. This work is supported by Grant-Aid for Encouragement of Young Scientist from the Ministry of Education, Science, Sports and Culture, Japan.

-
- ¹D. R. Nelson and H. S. Seung, Phys. Rev. B **39**, 9153 (1989).
²A. Houghton, R. A. Pelcovits, and A. Sudbø, Phys. Rev. B **40**, 6763 (1989).
³E. H. Brandt, Phys. Rev. Lett. **63**, 1106 (1989).
⁴M. P. A. Fisher, Phys. Rev. Lett. **62**, 1415 (1989); D. S. Fisher, M. P. A. Fisher, and D. A. Huse, Phys. Rev. B **43**, 130 (1991).
⁵D. R. Nelson and V. M. Vinokur, Phys. Rev. Lett. **68**, 2398 (1992).
⁶R. H. Koch *et al.*, Phys. Rev. Lett. **63**, 1511 (1989).
⁷P. L. Gammel, L. F. Schneemeyer, and D. J. Bishop, Phys. Rev. Lett. **66**, 953 (1991).
⁸C. Dekker, W. Eidelloth, and R. H. Koch, Phys. Rev. Lett. **68**, 3347 (1992).
⁹Y. Ando, H. Kubota, and S. Tanaka, Phys. Rev. Lett. **69**, 2851 (1992).
¹⁰J. Deak *et al.*, Phys. Rev. B **48**, 1337 (1993).
¹¹R. M. Silver, A. L. de Lozanne, and M. Thompson, IEEE Trans. Appl. Supercond. **3**, 1394 (1993).
¹²D. G. Xenikos, J.-T. Kim, and T. R. Lemberger, Phys. Rev. B **48**, 7742 (1993).
¹³P. J. M. Wöltgens *et al.*, Phys. Rev. B **48**, 16 826 (1993).
¹⁴H. Safar *et al.*, Phys. Rev. Lett. **72**, 1272 (1994).
¹⁵D. López *et al.*, Phys. Rev. Lett. **76**, 4034 (1996).
¹⁶D. T. Fuchs *et al.*, Phys. Rev. B **55**, R6156 (1997).
¹⁷D. López *et al.*, Phys. Rev. B **53**, R8895 (1996).
¹⁸E. F. Righi *et al.*, Phys. Rev. B **55**, 5663 (1997).
¹⁹W. S. Seow *et al.*, Phys. Rev. B **53**, 14 611 (1996).
²⁰D. R. Nelson and L. Radzihovsky, Phys. Rev. B **54**, R6845 (1996).
²¹P. Koorevaar *et al.*, Phys. Rev. B **47**, 934 (1993).
²²J. R. Clem, Phys. Rev. B **43**, 7837 (1991).
²³M. Tachiki and S. Takahashi, Solid State Commun. **72**, 1083 (1989).
²⁴A. I. Larkin and Yu. N. Ovchinnikov, J. Low Temp. Phys. **34**, 409 (1979).